

Revisiting the stratigraphic position of the Matuyama–Brunhes geomagnetic polarity boundary in Chinese loess

Chunsheng Jin, Qingsong Liu*

State Key Laboratory of Lithospheric Evolution, Institute of Geology and Geophysics, Chinese Academy of Sciences, Beijing, PR China, 100029

ARTICLE INFO

Article history:

Received 4 July 2010

Received in revised form 29 October 2010

Accepted 6 November 2010

Available online 11 November 2010

Keywords:

MB transitional polarity zone

Stratigraphy

Chinese loess

Marine sediments

ABSTRACT

It is commonly accepted that the climate records in Chinese loess can be correlated well with that in marine sediments. However, discrepancies for the stratigraphic position of paleomagnetic polarity reversal boundary seriously restrict an accurate teleconnection between these two archives. For example, the exact stratigraphic position of the whole Matuyama–Brunhes (MB) transitional polarity zone remains uncertain in Chinese loess. In this study, an accurate transitional zone of the MB reversal from the Mangshan profile, southeast margin of the Chinese Loess Plateau (CLP), was statistically determined using multiple subsets of parallel samples. By integrating results from the central CLP, the whole MB transitional zone is consistently located across the pedostratigraphic and climatostatigraphic transitional zones between S8 and L8 over a wide region of the CLP. This conclusion further supports that the paleosol unit S8 should be teleconnected to the marine oxygen isotope stage 19 rather than 21, and thus unambiguously supplies an accurate age control in constructing a new loess time scale.

Crown Copyright © 2010 Published by Elsevier B.V. All rights reserved.

1. Introduction

The alternating sequences of loess and paleosol from the Chinese Loess Plateau (CLP), considered as one of the most continuous terrestrial archives, preserve detailed paleomagnetic and paleoclimatic information for the last 2.6 Ma (e.g., An, 2000; Kukla and An, 1989; Liu, 1985; Liu and Ding, 1998), or even the last 22 Ma (Guo et al., 2002b). Further studies showed that the paleoclimatic signals can be correlated well with the marine oxygen isotope records (e.g., An et al., 2001; Deng et al., 2006; Ding et al., 2002; Heller and Evans, 1995; Heller and Liu, 1986). However, there is a longstanding controversy on correlations of paleomagnetic polarity reversal boundaries between these two archives. For example, the Matuyama–Brunhes (MB) boundary (MBB), the last geomagnetic reversal (~780 ka B.P.; Shackleton et al., 1990), as an important age control point, was commonly reported in loess horizon L8 (formed during a glacial period) in Chinese loess (e.g., Liu et al., 1988; Pan et al., 2002; Rutter et al., 1991; Sun et al., 1998; Yang et al., 2004; Zheng et al., 1992), whereas in marine sediments it was located in marine oxygen isotope stage 19 (MIS19, an interglacial stage) (e.g., Liu et al., 2008; Tauxe et al., 1996, and references therein). Large downward displacement of the MBB associated with post-depositional remanent magnetization acquisition lag (PDRM lock-in depth) has been proposed to explain this discrepancy by Zhou and Shackleton (1999).

They put forward that the MBB in Chinese loess should be located in the paleosol unit S7, not in the loess unit L8, and thus MIS19 would be tied to S7, not to S8. The corresponding PDRM lock-in depth ranges between a few tens and over 300 cm (Zhou and Shackleton, 1999). Spassov et al. (2003) have developed a lock-in model with two lock-in zones, where PDRM was superposed by chemical remanent magnetization, to support the large scale displacement of the MBB in Chinese loess. However, an inaccurate climatic boundary between L8 and S8 has been considered as the main cause for stratigraphic position confusion of the MBB by Liu et al. (2008). They revealed that the MBB at Lingtai and Zhaojiachuan sections were actually located in the upper part of S8.

The MBB at these two sections studied by Liu et al. (2008) are abrupt reversal boundaries due to a low sampling resolution (20 cm interval; Liu et al., 1988; Sun et al., 1998). Little is known about the duration and stratigraphic position of the whole MB transitional zone which lasts about 3–10 ka recorded in both marine sediments (e.g., Clement, 2004; Love and Mazaud, 1997, and references therein) and profiles from the other regions of the CLP (e.g., Spassov et al., 2001; Wang et al., 2006; Zhu et al., 1994a). Recently, Jin and Liu (2010) developed a new approach to statistically determine the exact MB transitional zone by measuring multiple subsets of parallel samples across the MBB. Compared to the stepwise pattern of the MBB investigated by Liu et al. (2008), the advantage of Jin and Liu's (2010) new approach makes it feasible to accurately determine the stratigraphic position of the whole MB transitional zone.

In addition, most of the reported MBB records clustered in the central CLP and little is known about that in the southeast periphery of

* Corresponding author. Tel.: +86 1082998365.

E-mail address: qslu@mail.iggcas.ac.cn (Q. Liu).

the CLP. The MBB records are essential for the southeastern CLP where sensitive to east-Asian summer monsoon. Therefore, in this study, by taking advantage of Jin and Liu's (2010) new approach, the Mangshan section (Fig. 1) will be investigated, which is situated at the southeast most margin and is far away from the central CLP. The stratigraphic position of an entire and an accurately recorded MB transitional zone in the Chinese loess will be addressed.

2. Sampling

The Mangshan section (34.9°N, 113.3°E) is located in the southeast margin of the CLP, about 380 km southeast of the famous Luochuan section in the hinterland of the CLP (Fig. 1). The thickness of the whole section is ~171 m, covering 12 paleosol horizons (S0–S11), interbedded with 11 loess horizons (L1–L11) (Fig. 2). The whole profile can well be correlated with what is commonly seen in the central CLP with exception of the top four extremely thick loess–paleosol beds, L1 to S2. The magnetic stratigraphy below S7 of this profile has been constructed by Zheng et al. (2007) using a single set of samples with relatively low stratigraphic resolution (sampling interval >20 cm). The MBB was approximately located in the lower part of L8 (Fig. 2). Nevertheless, the results of Zheng et al. (2007) provide useful background information for our high-resolution paleomagnetic studies.

In this study, paleomagnetic block samples (7×7×30 cm³) covering L8 and S8 were collected from the Mangshan section after removing weathered surface sediments. The samples were oriented *in situ* using a magnetic compass. We define the top of L8 as the zero position. The L8 and S8 beds are about 5 m thick in total. In the lab, the

block samples were sawn into 2.5 cm thick slices first, and then cut into 2×2×2 cm³ specimens. A total of 526 oriented specimens (five subsets of parallel samples) were obtained.

3. Experiments

The low field magnetic susceptibility (χ , *mass-specific) was measured using a Bartington MS2 susceptibility meter. Temperature-dependent susceptibility (χ - T) curves were measured using a KLY-3s Kappabridge equipped with a CS-3 high-temperature furnace going from room temperature up to 700 °C in an argon atmosphere (the flow rate is about 50 ml per minute) to avoid magnetic mineral alteration upon heating. Temperature-dependent saturation magnetization (M_s - T) curves were measured using a variable field translation balance system (VFTB). Samples for the M_s - T curves were heated in air in an applied field of 1 T. The temperature sweeping rate was 40 °C per minute. Hysteresis loops, isothermal remanent magnetization (IRM) acquisition curves, and back field demagnetization curves were measured with a Princeton Measurements vibrating sample magnetometer (VSM3900). The anisotropy of magnetic susceptibility (AMS) for oriented specimens was measured with a KLY-3s Kappabridge before thermal demagnetization.

Progressive thermal demagnetization of the natural remanent magnetization (NRM) was carried out from room temperature up to 585 °C using a Magnetic Measurements Thermal Demagnetizer (MMTD80) with a residual magnetic field of <10 nT. All remanences were measured using a 2 G Enterprises Model 760 cryogenic magnetometer installed in a magnetically shielded room (residual field <300 nT). One set of oriented samples between 102.5 and

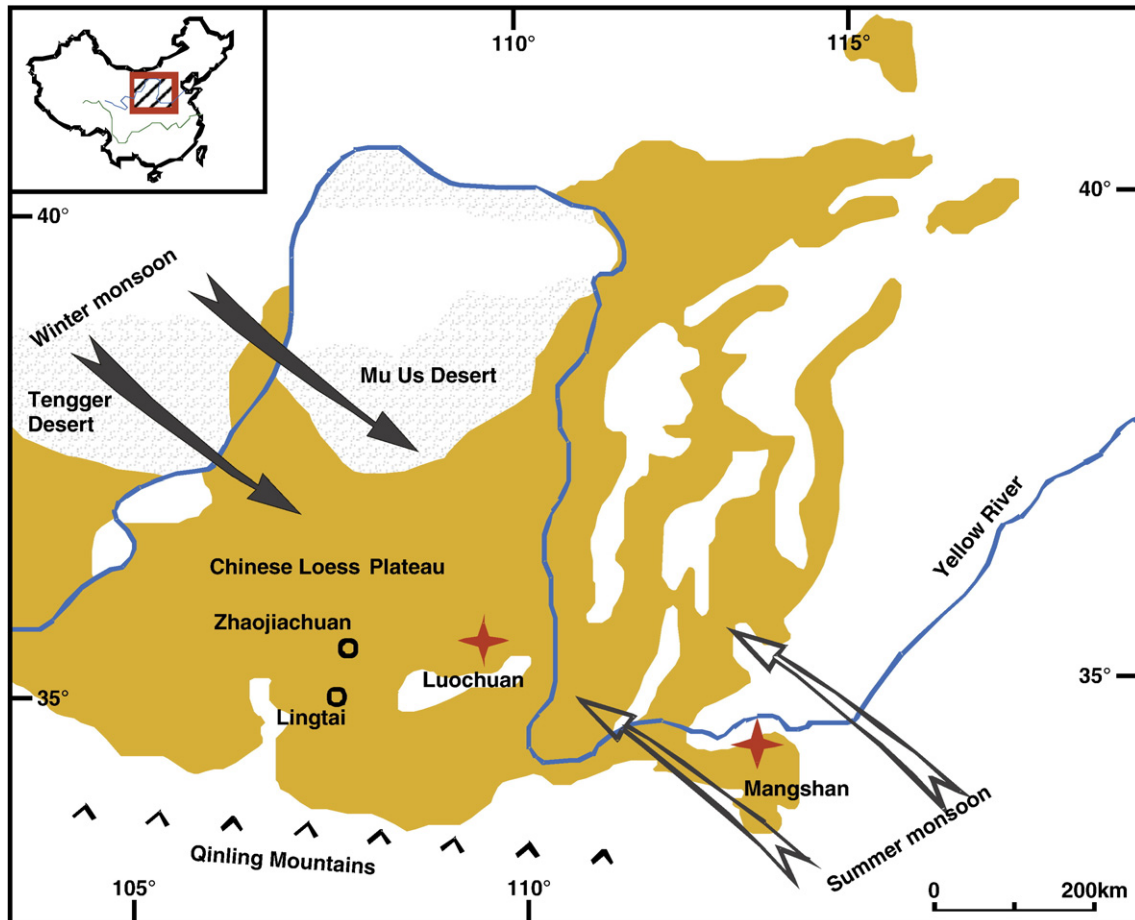


Fig. 1. A schematic map showing the distribution of the Chinese Loess Plateau and the location of the Mangshan, and Luochuan sections (stars), modified after Kukla (1987). Circles indicate other sections mentioned in the text.

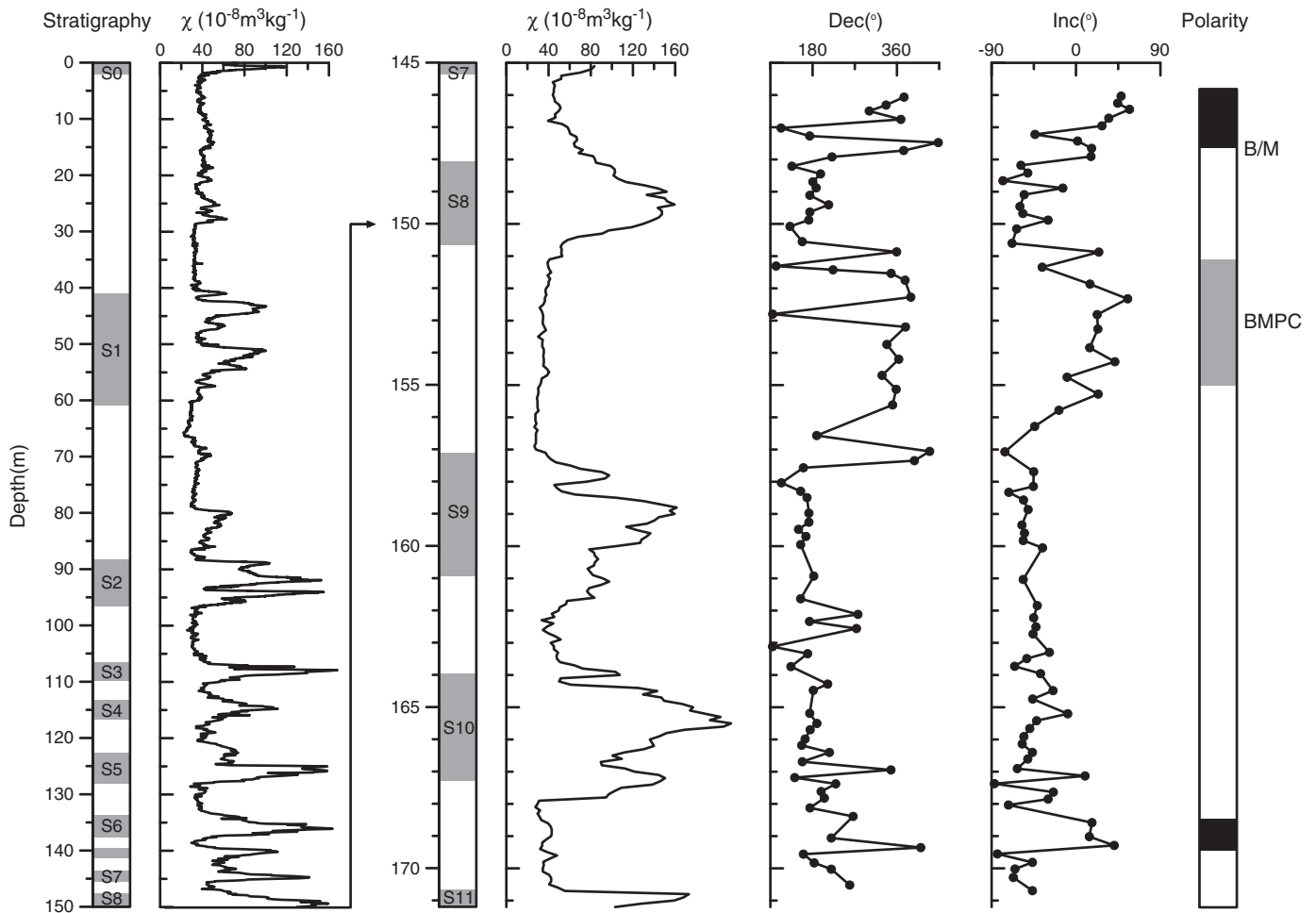


Fig. 2. Pedostratigraphy, magnetic susceptibility, and magnetostratigraphy for Mangshan section (Zheng et al., 2007). Dec, declination of characteristic remanent magnetization (ChRM). Inc, inclination of ChRM.

390 cm was first demagnetized to locate the MBB. Then the other four parallel sample sets (A–D) between 130 and 280 cm were thermally demagnetized to define the exact position of the MB transitional zone.

The colour reflectance of bulk samples across the MBB from both the Mangshan and Luochuan sections was measured using a handheld Minolta-CM2002 spectrophotometer. We adopt red–green chromaticity a^* to identify the stratum (refers to colour- a^*). Grain size was measured with a SALD-3001 laser diffraction particle analyzer. Ultrasonic pretreatment with the addition of 20% $(\text{NaPO}_3)_6$ solution was used to disaggregate the samples before measurement.

4. Results

4.1. Rock magnetic results

Stepwise acquisition of the IRM curves climbs quickly before 200 mT and reaches approximate saturation at about 300 mT (Fig. 3a), indicating existence of dominant low coercivity magnetic carriers (e.g., magnetite, maghemite). The IRM curves increase faintly after 300 mT until 2 T, indicating the presence of hard magnetic minerals (e.g., hematite, probably goethite) (Yang et al., 2010). SIRM for samples from the paleosol unit is evidently higher than that from the loess layer.

After the removal of a significant paramagnetic contribution, hysteresis loops for all the samples show similar characteristics. They are almost closed before 300 mT (Fig. 3b), indicating existence of soft magnetic minerals (e.g., magnetite, maghemite) (Deng et al., 2004),

consistent with results of the IRM curves. Loops for samples from S8 display weakly wasp-waisted shape (Roberts et al., 1995).

The χ - T curves are almost reversible except the one at 207.5 cm. The heating curves for all the samples are similar in shape. Upon heating, the χ increases slowly below 200 °C, and decreases steadily between 200 and 400 °C and sharply after 400 °C. The χ - T curves show a major inflexion at about 585 °C upon heating, displaying the Curie point of magnetite (Fig. 3c). The slightly decreases over 200–400 °C are commonly considered to be maghemite signals with conversion to weakly magnetic hematite (Deng et al., 2000, 2004, 2006; Deng, 2008; Liu et al., 2005b).

The inflexions in the M_s - T curves at about 580 °C further suggest the presence of magnetite (Fig. 3d). Maghemite is also identifiable from the kink over 300–450 °C (Liu et al., 2003; Wang et al., 2005; Yang et al., 2008, 2010). Hematite signals are weakly displayed in both the M_s - T curves and the χ - T curves which slightly decrease above 600 °C.

Hysteresis parameters ratios, M_{rs}/M_s , B_{cr}/B_c (termed Day plot; Day et al., 1977), were plotted on a revised version (Dunlop, 2002). All ratios cluster closely in the pseudo-single-domain (PSD) grain size region (Fig. 4). This indicates that the mean grain size of magnetic minerals in samples is rather uniform across the sampled interval.

4.2. AMS results

Zhu et al. (2004) found that the AMS of the Chinese loess/paleosols is essentially controlled by ferromagnetic components, and effects from paramagnetic components are negligible. Constrained by the

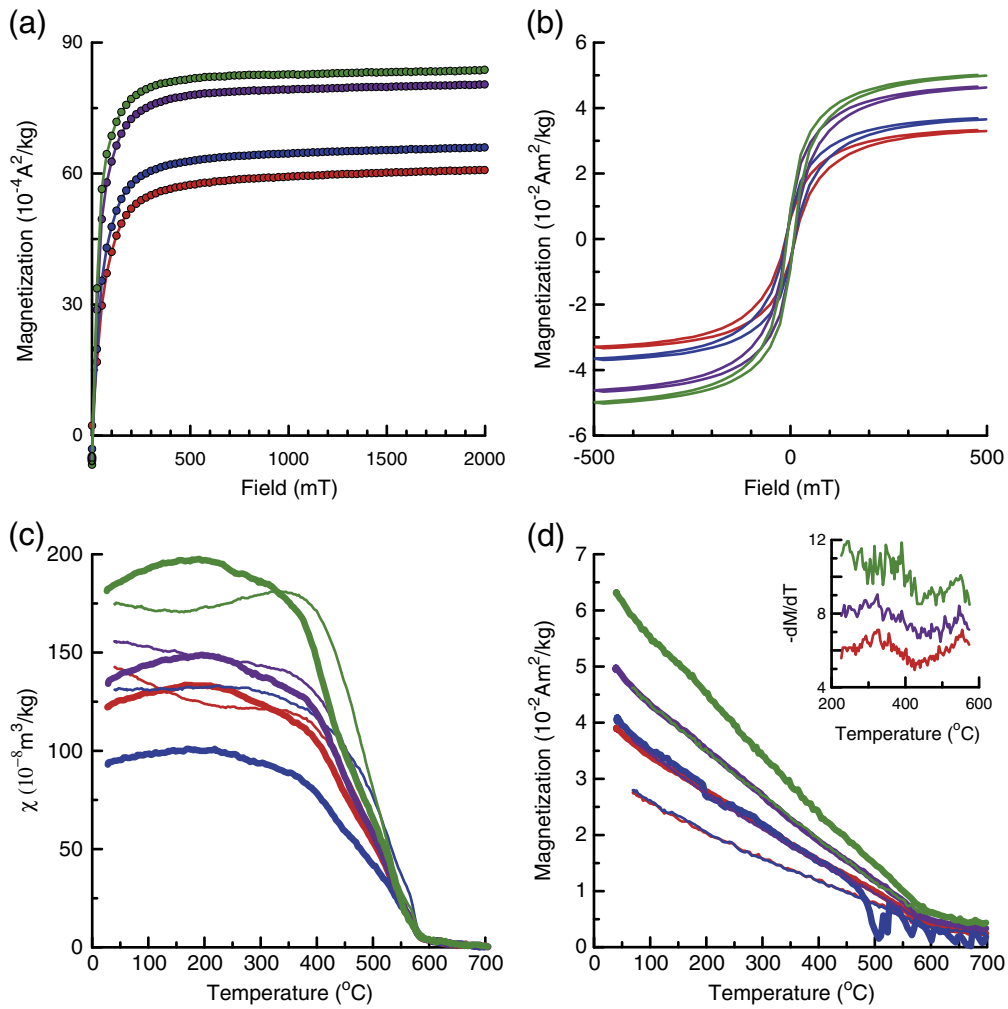


Fig. 3. Rock magnetism results for the Mangshan section. (a) Isothermal remanent magnetization acquisition curves. (b) Hysteresis loops, after subtraction of the paramagnetic contribution. (c) Temperature-dependent susceptibility curves. (d) Temperature-dependent magnetization (M_s - T curves). Thick (thin) lines mean heating and cooling, respectively. $-dM/dT$ ($10^{-3} \text{ Am}^2 \text{ kg}^{-1} \text{ } ^\circ\text{C}^{-1}$) indicates the first derivative of M_s - T curves. The red, blue, purple, and grass green lines represent samples at 117.5, 207.5, 297.5, 352.5 cm, respectively.

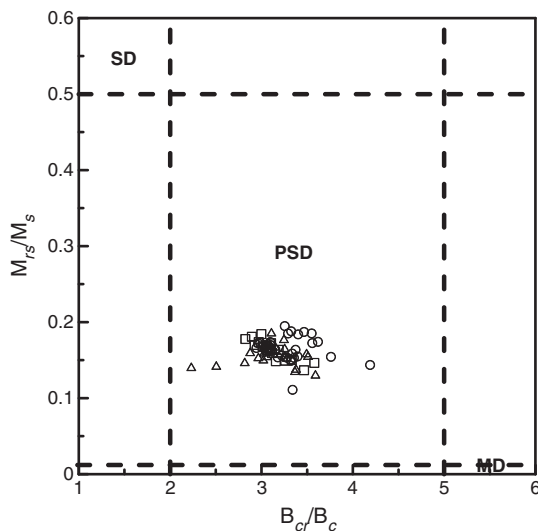


Fig. 4. Hysteresis ratios plotted on a revised Day plot (Day et al., 1977; Dunlop, 2002). Triangles, squares, circles represent samples in the Brunhes zone, Matuyama-Brunhes transitional zone, Matuyama zone, respectively.

field-impressed AMS and the anisotropy of anhysteretic remanent magnetization (AARM) of the Chinese loess, Liu et al. (2005c) further put forward that magnetic lineation is determined by coarse-grained magnetite, and thus can be used to indicate the paleowind direction. AARM often has higher anisotropy than AMS, but to the first order, it seems that they are linearly correlated (Liu et al., 2005c). Therefore, the AMS results, especially the inclination of the maximum susceptibility axis and minimum susceptibility axis, have been widely used in loess studies to detect possible disturbance of the original sediment fabric and to test the reliability of NRM recording (e.g., Guo et al., 2001, 2002a; Liu et al., 1988, 2005a; Wang et al., 2005, 2010; Yang et al., 2007, 2010; Zhu et al., 1994a, 1999, 2004).

The equal-area stereographic projections of the AMS principal directions for the oriented samples are shown in Fig. 5. The inclinations of the maximum susceptibility axes are $<15^\circ$ (96% $<10^\circ$), approximately parallel to the horizontal plane. The inclinations of the minimum susceptibility axes are $>75^\circ$ (86% $>80^\circ$), perpendicular to the horizontal plane. Such an oblate AMS pattern represents a primary depositional sediment fabric without apparent disorder and disturbance.

4.3. Paleomagnetic results

The orthogonal projections (Zijderveld, 1967) for four representative specimens show normal (Fig. 6a, c) and reverse (Fig. 6b, d)

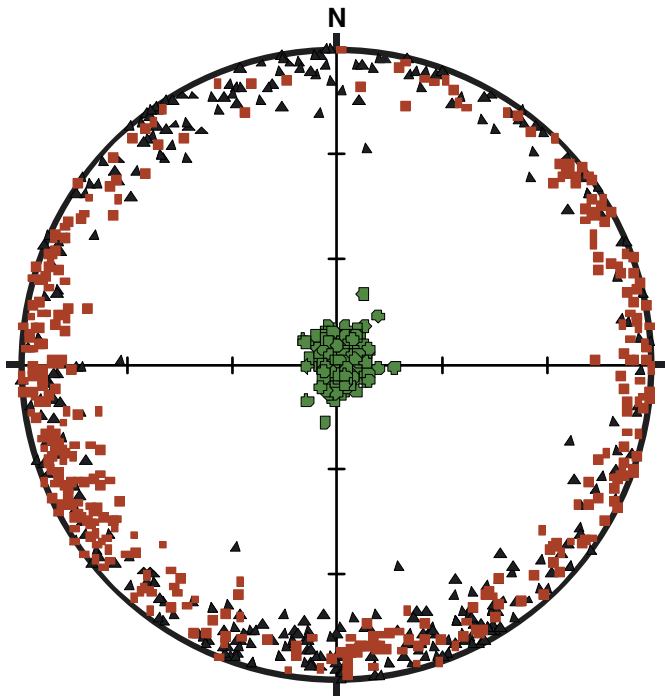


Fig. 5. AMS principal directions in an equal-area stereographic projection. Squares, triangles, and circles represent maximum, intermediate, and minimum-susceptibility axis, respectively.

polarity, respectively. There are two magnetic components in the NRM demagnetization curves. The low temperature component (<300 °C) of NRM was commonly considered as viscous remanent magnetization (VRM) and could be eliminated after about 250–300 °C thermal treatment (e.g., Deng, 2008; Heller and Liu, 1982; Pan et al., 2001; Zhu et al., 1994a). A characteristic remanent magnetization (ChRM) was isolated successively for most of the samples (77%) between 300 and 550 °C using principal component analysis calculated by the least-squares fitting technique of Kirschvink (1980). Associated with the rock magnetic results, the ChRMs are carried pre-dominantly by PSD magnetite, which is considered to be of eolian origin. This is consistent with previous studies (e.g., Heller and Liu, 1982, 1984; Pan et al., 2002; Yang et al., 2010; Zhu et al., 1994a). An abnormal paleomagnetic polarity zone can be unambiguously determined by the five subsets of parallel samples in the 170–255 cm interval (Fig. 7).

4.4. Climatology proxies

The colour-*a** has been considered as an efficient proxy for the weathering intensity of loess and been used in pedostratigraphy division (Yang and Ding, 2003). Magnetic susceptibility and median grain size are commonly accepted as proxies for the east-Asian summer and winter monsoons, respectively (An, 2000; An et al., 2001; Ding et al., 2002; Liu and Ding, 1998). The colour-*a** and magnetic susceptibility values are higher in the paleosol unit than in the loess unit in both the Mangshan and Luochuan sections, whereas the median grain size displays a contrary behavior (Fig. 8).

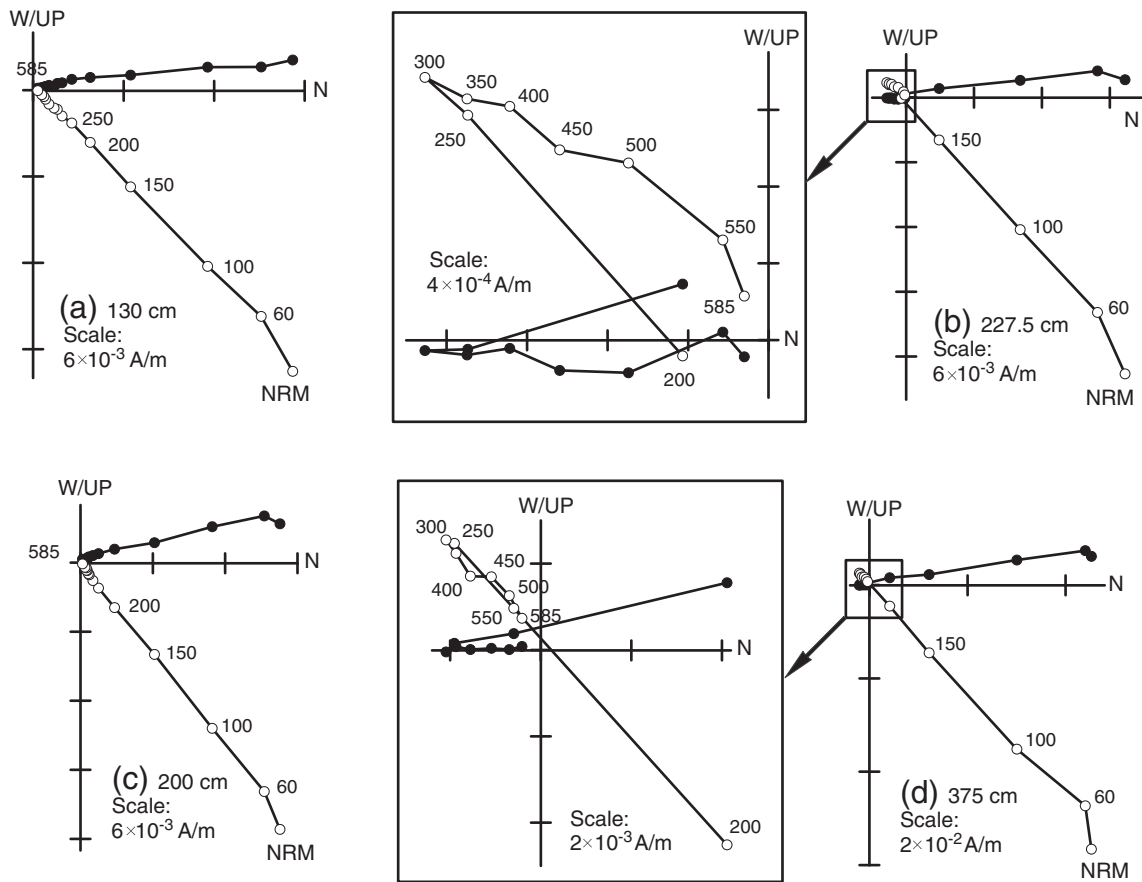


Fig. 6. Orthogonal projections of progressive thermal demagnetization of natural remanent magnetization (NRM) for representative specimens at the Mangshan section in (a) the Brunhes zone, (b, c) the Matuyama–Brunhes transitional zone, and (d) the Matuyama zone. Solid (open) circles represent projections onto the horizontal (vertical) plane. Demagnetization temperature is given in degrees Celsius.

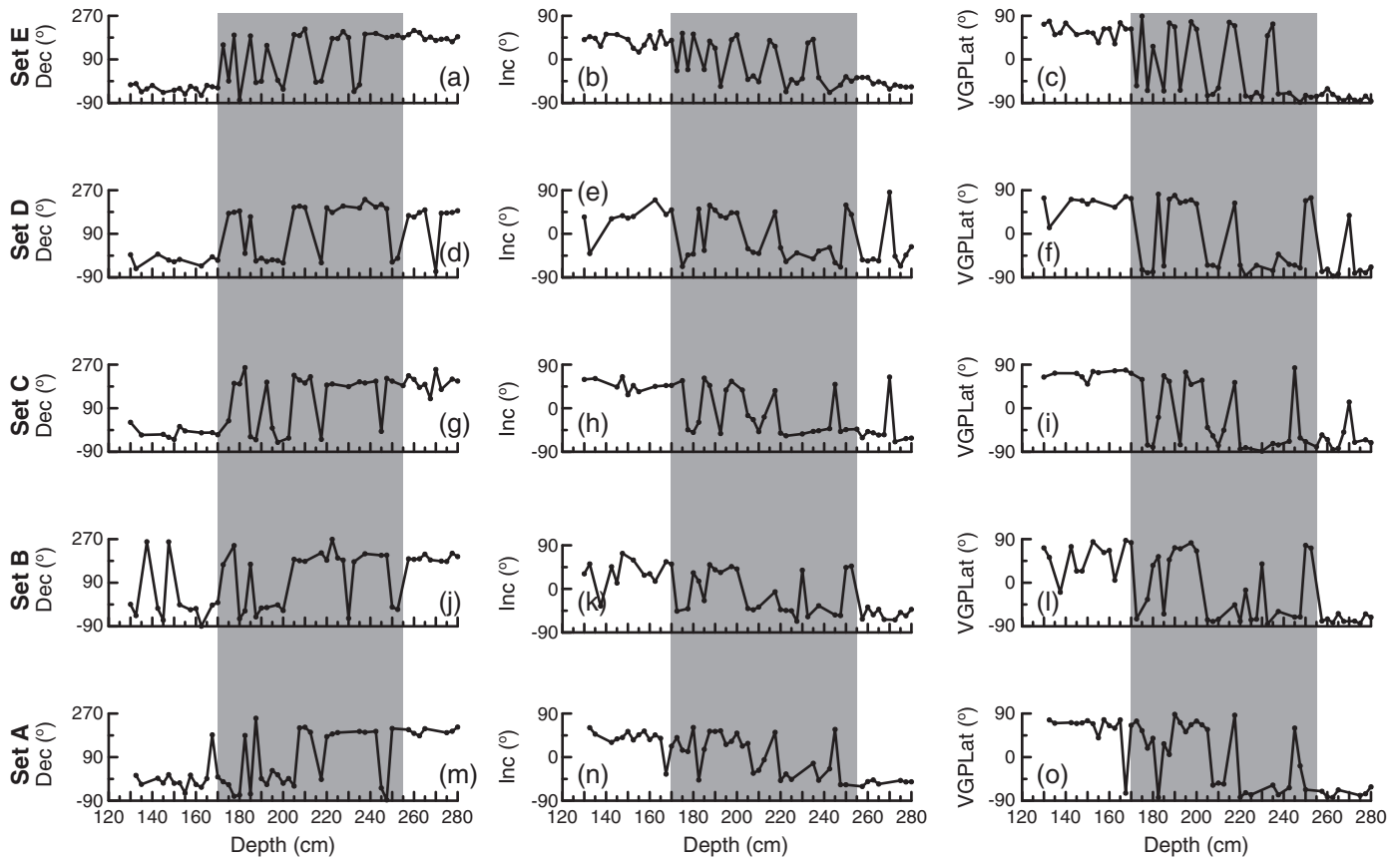


Fig. 7. Magnetic stratigraphy of L8 and S8 in the 130–280 cm interval from the Mangshan section. Sets A–E are parallel samples. Dec, Inc, virtual geomagnetic pole latitude (VGP Lat) are shown in the left, middle, and right columns, respectively. Directional anomalies are shaded.

5. Discussion

Most previous studies on the paleomagnetic records from the Chinese loess relied on only single set of samples (Liu et al., 1988; Pan et al., 2002; Rutter et al., 1991; Sun et al., 1998; Yang et al., 2004; Zheng et al., 1992). Such an approach cannot determine the fidelity of the paleomagnetic wiggles represented by only a few samples (e.g., Spassov et al., 2001; Sun et al., 1993; Yang et al., 2010; Yue et al., 1990), and thus potential ambiguities exist when defining the polarity transitional boundary of paleomagnetic reversals. This study confirmed the ideas of Jin and Liu (2010) that the ChRMs of multiple subsets of parallel samples are inconsistent during the transition, whereas keeping agreement outside the transition (Fig. 7). This phenomenon has been attributed to the low efficient alignment of detrital magnetite along with a weak paleomagnetic field during a polarity transition period (Jin and Liu, 2010). An alternative interpretation of the complicated NRM records from the Chinese loess is due to effects from lock-in processes (Zhou and Shackleton, 1999). However, such a model cannot be applied to the coeval parallel samples. In addition, more studies support a small NRM lock-in depth in Chinese loess (e.g., Pan et al., 2002; Wang et al., 2006; Yang et al., 2008, 2010; Zhu et al., 1994a, 1998, 2006). Sediment redeposition experiments suggest that the capability of deposited loess dust to acquire a PDRM is enhanced with water content (Zhao and Roberts, 2010). Magnetic particles as ChRM carriers in the deposited dusts can be fixed permanently along the ambient field after the initial wetting (Wang and Løvlie, 2010). The moisture in the sedimentary environment is associated with the rainfall in the CLP and results in a shallow lock-in model, which is also evident in the short-period paleomagnetic events recorded in Chinese loess, such as magnetic excursions (e.g., Fang et al., 1997; Pan et al., 2002; Yang et al., 2007; Zheng et al., 1995; Zhu et al., 1994b, 1999, 2006, 2007). Thus, the

downward displacements of the polarity boundaries in loess may be limited to only several centimeters due to high sediment rates and shallow NRM lock-in depth (Liu et al., 2008), associated with a limited surface mixing layer (<10 cm) (Sun et al., 2010).

Although the detailed morphology for a paleomagnetic polarity transitional field cannot be accurately defined at these two loess sites, the MB transitional zones have been statistically and less ambiguously determined, such as the 170–255 cm interval at Mangshan section. Because the deposition rate of Chinese loess differs significantly among different profiles, the thickness of the MB transitional zone should be also different. Therefore, in order to compare the duration of the MB transitional zone recorded at different profiles, the ratio ($T_{\text{MBB}}/T_{\text{L8+S8}}$, where T indicates the thickness) of the thickness of the MB transitional zone to the total thickness of L8 and S8 is defined. $T_{\text{L8+S8}}$ values for the Luochuan and Mangshan profiles are ~290 and ~500 cm, respectively. The corresponding T_{MBB} values are 47.5 and 85 cm, respectively. Therefore, the ratios of $T_{\text{MBB}}/T_{\text{L8+S8}}$ for these two profiles are 0.164 and 0.170, respectively, which indicates a rather consistent duration of the MB reversal recorded in these two areas.

It is difficult to recognize the precise pedomatigraphic boundary between S8 and L8 in field, but it can be more accurately defined by multiple proxies (soil structure and colour, magnetic susceptibility, and the median grain size) in both the Mangshan and Luochuan sections (Fig. 8). In addition, grain size is superior to susceptibility because the latter is controlled more by the amount of the local precipitation (Liu et al., 2005a; Maher and Thompson, 1995). Apparently, the whole MB transitional zone is not singly recorded in a loess unit or a paleosol unit, but in the interval which transgresses from the paleosol unit S8 into the loess unit L8 (shaded in Fig. 8).

The magnetic behavior around the MB reversal at the Mangshan section resembles that in the Luochuan region (Jin and Liu, 2010),

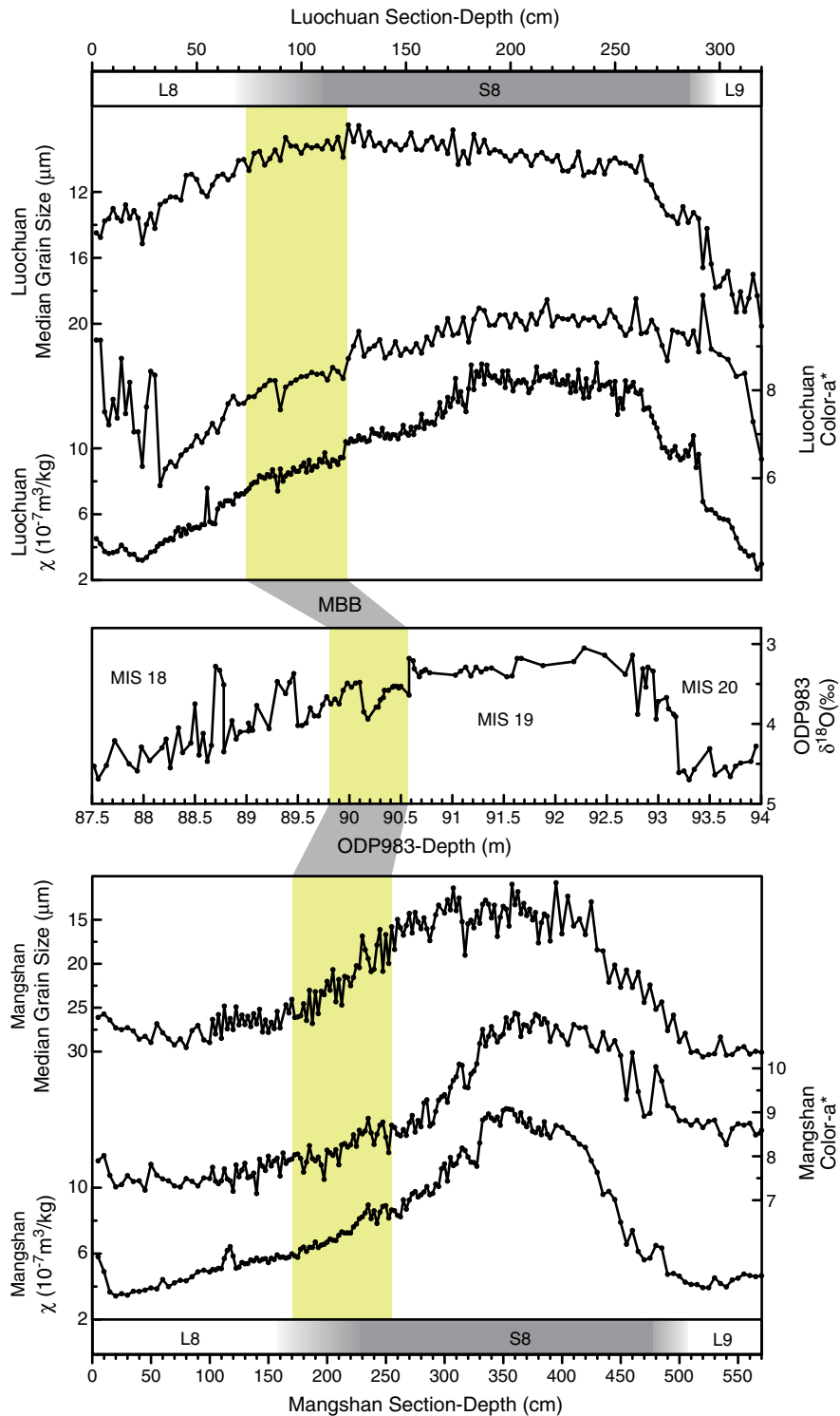


Fig. 8. Stratigraphic correlations between the Luochuan section, Mangshan section, and benthic foraminiferal $\delta^{18}\text{O}$ for ODP983 (data from Channell and Kleiven, 2000). The Matuyama–Brunhes boundary (MBB) is shaded. The MBB and low-field magnetic susceptibility (χ) for the Luochuan section are from Jin and Liu (2010). The MBB for ODP983 was adjusted 20 cm upward according to Liu et al. (2008).

indicating a possible spatial comparability of paleomagnetic recording pattern in Chinese loess, although pedogenesis is enhanced in the southeast margin of the CLP as compared to the central areas (Wang et al., 2006). By combining results from the central CLP (Heller and Liu, 1982; Jin and Liu, 2010; Yang et al., 2010) and from the southeast margin of the CLP in this study, the MBB is unambiguously recorded across the stratigraphic transition boundary between S8 and L8 over a wide range of the Chinese Loess Plateau. In marine sediments, owing

to decimeter scale PDRM lock-in depth (deMenocal et al., 1990; Liu et al., 2008; Roberts and Winkhofer, 2004), the MBB is most likely to lie in the late MIS19 (Liu et al., 2008), not in the middle of MIS19 as suggested by Lisiecki and Raymo (2005). This case is consistent with the MBB records in Chinese loess with a stratigraphic position partly in the upper part of S8 (formed during an interglacial period). Therefore we further conclude that S8 should correlate to MIS19, and not to MIS21 as proposed by Zhou and Shackleton (1999), and thus

the chronological framework for the Chinese loess–paleosol sequences based on the strongly delayed lock-in models should be reconsidered.

6. Conclusions

Compared to previous studies, the major contribution of this study is that the stratigraphic position of the whole MB transitional zone is consistently determined over a large spatial region from the center to the southeast margin of the CLP. Based on pedostratigraphic and climatostratigraphic division, the MB transitional zone is not singly recorded in the loess unit L8 or the paleosol unit S8, but in the stratigraphic transition zone which transgresses from S8 into L8. This is important for constructing a new chronology framework for the Chinese loess–paleosol sequences. It should be considered as a routine approach to determine the accurate position of the MBB in Chinese loess using sets of parallel samples.

Acknowledgements

This study was supported by the National Natural Science Foundation of China (grants 41004023, 41025013, and 40821091) and the Chinese Academy of Sciences. Q. Liu acknowledges further support from the 100-talent Program of the Chinese Academy of Sciences. We gratefully acknowledge two anonymous journal reviewers for their critical comments and for helping improving the language.

References

- An, Z.S., 2000. The history and variability of the East Asian paleomonsoon climate. *Quaternary Science Reviews* 19, 171–187.
- An, Z.S., Kutzbach, J.E., Prell, W.L., Porter, S.C., 2001. Evolution of Asian monsoons and phased uplift of the Himalaya–Tibetan plateau since Late Miocene times. *Nature* 411, 62–66.
- Channell, J.E.T., Kleiven, H.F., 2000. Geomagnetic palaeointensities and astrochronological ages for the Matuyama–Brunhes boundary and the boundaries of the Jaramillo Subchron: palaeomagnetic and oxygen isotope records from ODP Site 983. *Philosophical Transactions of the Royal Society of London. Series A* 358, 1027–1047.
- Clement, B.M., 2004. Dependence of the duration of geomagnetic polarity reversals on site latitude. *Nature* 428, 637–640.
- Day, R., Fuller, M., Schmidt, V.A., 1977. Hysteresis properties of titanomagnetite: grain-size and compositional dependence. *Physics of the Earth and Planetary Interiors* 13, 260–266.
- deMenocal, P.B., Ruddiman, W.F., Kent, D.V., 1990. Depth of post-depositional remanence acquisition in deep-sea sediments: a case study of the Brunhes–Matuyama reversal and oxygen isotopic Stage 19.1. *Earth and Planetary Science Letters* 99, 1–13.
- Deng, C.L., 2008. Paleomagnetic and mineral magnetic investigation of the Baicaoyuan loess–paleosol sequence of the western Chinese Loess Plateau over the last glacial–interglacial cycle and its geological implications. *Geochemistry, Geophysics, Geosystems* 9 (4), Q04034. doi:10.1029/2007GC001928.
- Deng, C.L., Zhu, R.X., Verosub, K.L., Singer, M.J., Yuan, B.Y., 2000. Paleoclimatic significance of the temperature-dependent susceptibility of Holocene loess along a NW–SE transect in the Chinese loess plateau. *Geophysical Research Letters* 27 (22), 3715–3718.
- Deng, C.L., Zhu, R.X., Verosub, K.L., Singer, M.J., Vidic, N.J., 2004. Mineral magnetic properties of loess/paleosol couplets of the central loess plateau of China over the last 1.2 Myr. *Journal of Geophysical Research* 109, B01103. doi:10.1029/2003JB002532.
- Deng, C.L., Shaw, J., Liu, Q.S., Pan, Y.X., Zhu, R.X., 2006. Mineral magnetic variation of the Jingbian loess/paleosol sequence in the northern Loess Plateau of China: implications for Quaternary development of Asian aridification and cooling. *Earth and Planetary Science Letters* 241 (1–2), 248–259.
- Ding, Z.L., Derbyshire, E., Yang, S.L., Yu, Z.W., Xiong, S.F., 2002. Stacked 2.6-Ma grain size record from the Chinese loess based on five sections and correlation with the deep-sea $\delta^{18}\text{O}$ record. *Paleoceanography* 17 (3), 1033. doi:10.1029/2001PA000725.
- Dunlop, D.J., 2002. Theory and application of the Day plot (M_{rs}/M_s versus H_{cr}/H_c) 1. Theoretical curves and tests using titanomagnetite data. *Journal of Geophysical Research* 107 (B3), 2056. doi:10.1029/2001JB000486.
- Fang, X.M., Li, J.J., derVoo, R.V., Niocaill, C.M., Dai, X.R., Kemp, R.A., Derbyshire, E., Cao, J.X., Wang, J.M., Wang, G., 1997. A record of the Blake Event during the last interglacial paleosol in the western Loess Plateau of China. *Earth and Planetary Science Letters* 146, 73–82.
- Guo, B., Zhu, R.X., Florindo, F., Pan, Y.X., Yue, L.P., 2001. Pedogenesis affecting the Matuyama–Brunhes polarity transition recorded in Chinese loess. *Chinese Science Bulletin* 46, 975–981.
- Guo, B., Zhu, R.X., Florindo, F., Ding, Z.L., Sun, J.M., 2002a. A short, reverse polarity interval within the Jaramillo subchron: evidence from the Jingbian section, northern Chinese Loess Plateau. *Journal of Geophysical Research* 107. doi:10.1029/2001JB000706.
- Guo, Z.T., Ruddiman, W.F., Hao, Q.Z., Wu, H.B., Qiao, Y.S., Zhu, R.X., Peng, S.Z., Wei, J.J., Yuan, B.Y., Liu, T.S., 2002b. Onset of Asian desertification by 22 Myr ago inferred from loess deposits in China. *Nature* 416, 159–163.
- Heller, F., Evans, M.E., 1995. Loess magnetism. *Reviews of Geophysics* 33, 211–240.
- Heller, F., Liu, T.S., 1982. Magnetostratigraphical dating of loess deposits in China. *Nature* 300, 431–433.
- Heller, F., Liu, T.S., 1984. Magnetism of Chinese loess deposits. *Geophysical Journal of the Royal Astronomical Society* 77, 125–141.
- Heller, F., Liu, T.S., 1986. Palaeoclimatic and sedimentary history from magnetic susceptibility of loess in China. *Geophysical Research Letters* 13 (11), 1169–1172.
- Jin, C.S., Liu, Q.S., 2010. Reliability of the natural remanent magnetization recorded in Chinese loess. *Journal of Geophysical Research* 115, B04103. doi:10.1029/2009JB006703.
- Kirschvink, J.L., 1980. The least-squares line and plane and the analysis of palaeomagnetic data. *Geophysical Journal of the Royal Astronomical Society* 62, 699–718.
- Kukla, G., 1987. Loess stratigraphy in central China. *Quaternary Science Reviews* 6, 191–219.
- Kukla, G., An, Z.S., 1989. Loess stratigraphy in central China. *Palaeogeography, Palaeoclimatology, Palaeoecology* 72, 203–225.
- Lisiecki, L.E., Raymo, M.E., 2005. A Pliocene–Pleistocene stack of 57 globally distributed benthic $\delta^{18}\text{O}$ records. *Paleoceanography* 20, PA1003. doi:10.1029/2004PA001071.
- Liu, T.S., 1985. Loess and the Environment. China Ocean Press, Beijing.
- Liu, T.S., Ding, Z.L., 1998. Chinese loess and the paleomonsoon. *Annual Review of Earth and Planetary Sciences* 26, 111–145.
- Liu, X.M., Liu, T.S., Xu, T.C., Liu, C., Chen, M.Y., 1988. The Chinese loess in Xifeng, I. The primary study on magnetostratigraphy of a loess profile in Xifeng area, Gansu province. *Geophysical Journal* 92, 345–348.
- Liu, Q.S., Banerjee, S.K., Jackson, M.J., 2003. An integrated study of the grain-size-dependent magnetic mineralogy of the Chinese loess/paleosol and its environmental significance. *Journal of Geophysical Research* 108 (B9), 2437. doi:10.1029/2002JB002264.
- Liu, Q.S., Banerjee, S.K., Jackson, M.J., Deng, C.L., Pan, Y.X., Zhu, R.X., 2005a. Inter-profile correlation of the Chinese loess/paleosol sequences during Marine Oxygen Isotope Stage 5 and indications of pedogenesis. *Quaternary Science Reviews* 24 (1–2), 195–210.
- Liu, Q.S., Deng, C.L., Yu, Y., Yorrent, J., Jackson, M.J., Banerjee, S.K., Zhu, R.X., 2005b. Temperature dependence of magnetic susceptibility in an argon environment: implications for pedogenesis of Chinese loess/paleosols. *Geophysical Journal International* 161, 102–112.
- Liu, Q.S., Yu, Y.J., Deng, C.L., Pan, Y.X., Zhu, R.X., 2005c. Enhancing weak magnetic fabrics using field-impressed anisotropy: application to the Chinese loess. *Geophysical Journal International* 162, 381–389.
- Liu, Q.S., Roberts, A.P., Rohling, E.J., Zhu, R.X., Sun, Y.B., 2008. Post-depositional remanent magnetization lock-in and the location of the Matuyama–Brunhes geomagnetic reversal boundary in marine and Chinese loess sequences. *Earth and Planetary Science Letters* 275, 102–110.
- Love, J.J., Mazaud, A., 1997. A database for the Matuyama–Brunhes magnetic reversal. *Physics of the Earth and Planetary Interiors* 103, 207–245.
- Maher, B.A., Thompson, R., 1995. Paleorainfall reconstructions from pedogenic magnetic susceptibility variations in the Chinese loess and paleosols. *Quaternary Research* 44, 383–391.
- Pan, Y.X., Zhu, R.X., Shaw, J., Liu, Q.S., Guo, B., 2001. Can relative paleointensities be determined from the normalized magnetization of the wind-blown loess of China? *Journal of Geophysical Research* 106 (B9), 19221–19232.
- Pan, Y.X., Zhu, R.X., Liu, Q.S., Guo, B., Yue, L.P., Wu, H.N., 2002. Geomagnetic episodes of the last 1.2 Myr recorded in Chinese loess. *Geophysical Research Letters* 29 (8), 1231–1234.
- Roberts, A.P., Winklhofer, M., 2004. Why are geomagnetic excursions not always recorded in sediments? Constraints from post-depositional remanent magnetization lock-in modelling. *Earth and Planetary Science Letters* 227 (3–4), 345–359.
- Roberts, A.P., Cui, Y.L., Verosub, K.L., 1995. Wasp-waisted hysteresis loops: Mineral magnetic characteristics and discrimination of components in mixed magnetic systems. *Journal of Geophysical Research* 100 (B9), 17909–17924.
- Rutter, N., Ding, Z.L., Evans, M.E., Liu, T.S., 1991. Baoji-type pedostratigraphic section, loess plateau, north-central China. *Quaternary Science Reviews* 10, 1–22.
- Shackleton, N.J., Berger, A., Peltier, W.R., 1990. An alternative astronomical calibration of the lower Pleistocene timescale based on ODP Site 677. *Transactions of The Royal Society of Edinburgh: Earth Sciences* 81, 251–261.
- Spassov, S., Heller, F., Evans, M.E., Yue, L.P., Ding, Z.L., 2001. The Matuyama/Brunhes geomagnetic polarity transition at Lingtai and Baoji, Chinese Loess Plateau. *Physics and Chemistry of the Earth (A)* 26 (11–12), 899–904.
- Spassov, S., Heller, F., Evans, M.E., Yue, L.P., Dobeneck, T.v., 2003. A lock-in model for the complex Matuyama–Brunhes boundary record of the loess/paleosol sequence at Lingtai (Central Chinese Loess Plateau). *Geophysical Journal International* 155, 350–366.
- Sun, D.H., Shaw, J., An, Z.S., Rolph, T., 1993. Matuyama/Brunhes(M/B) transition recorded in Chinese loess. *Journal of Geomagnetism and Geoelectricity* 45, 319–330.
- Sun, D.H., Shaw, J., An, Z.S., Cheng, M.Y., Yue, L.P., 1998. Magnetostratigraphy and paleoclimatic interpretation of a continuous 7.2 Ma Cenozoic eolian sediments from the Chinese Loess Plateau. *Geophysical Research Letters* 25 (1), 85–88.
- Sun, Y.B., Wang, X.L., Liu, Q.S., Clemens, S.C., 2010. Impacts of post-depositional processes on rapid monsoon signals recorded by the last glacial loess deposits of northern China. *Earth and Planetary Science Letters* 289, 171–179.

- Tauxe, L., Herbert, T., Shackleton, N.J., Kok, Y.S., 1996. Astronomical calibration of the Matuyama–Brunhes boundary: Consequences for magnetic remanence acquisition in marine carbonates and the Asian loess sequences. *Earth and Planetary Science Letters* 140, 133–146.
- Wang, R.H., Løvlie, R., 2010. Subaerial and subaqueous deposition of loess: experimental assessment of detrital remanent magnetization in Chinese loess. *Earth and Planetary Science Letters* 298, 394–404.
- Wang, X.S., Løvlie, R., Yang, Z.Y., Pei, J.L., Zhao, Z.Z., Sun, Z.M., 2005. Remagnetization of Quaternary eolian deposits: a case study from SE Chinese Loess Plateau. *Geochemistry, Geophysics, Geosystems* 6 (6), Q06H18. doi:10.1029/2004GC000901.
- Wang, X.S., Yang, Z.Y., Løvlie, R., Sun, Z.M., Pei, J.L., 2006. A magnetostratigraphic reassessment of correlation between Chinese loess and marine oxygen isotope records over the last 1.1 Ma. *Physics of the Earth and Planetary Interiors* 159, 109–117.
- Wang, D.J., Wang, Y.C., Han, J.T., Duan, M.G., Shan, J.Z., Liu, T.S., 2010. Geomagnetic anomalies recorded in L9 of the Songjiadian loess section in southeastern Chinese Loess Plateau. *Chinese Science Bulletin* 55, 520–529.
- Yang, S.L., Ding, Z.L., 2003. Color reflectance of Chinese loess and its implications for climate gradient changes during the last two glacial–interglacial cycles. *Geophysical Research Letters* 30 (20), 2058. doi:10.1029/2003GL018346.
- Yang, T.S., Hyodo, M., Yang, Z.Y., Fu, J.L., 2004. Evidence for the Kamikatsura and Santa Rosa excursions recorded in eolian deposits from the southern Chinese Loess Plateau. *Journal of Geophysical Research* 109, B12105. doi:10.1029/2004JB002966.
- Yang, T.S., Hyodo, M., Yang, Z.Y., Fu, J.L., 2007. Two geomagnetic excursions during the Brunhes chron recorded in Chinese loess–palaeosol sediments. *Geophysical Journal International* 171, 104–114.
- Yang, T.S., Hyodo, M., Yang, Z.Y., Ding, L., Li, H.D., Fu, J.L., Wang, S.B., Wang, H.W., Mishima, T., 2008. Latest Olduvai short-lived reversal episodes recorded in Chinese loess. *Journal of Geophysical Research* 113, B05103. doi:10.1029/2007JB005264.
- Yang, T.S., Hyodo, M., Yang, Z.Y., Li, H.D., Maeda, M., 2010. Multiple rapid polarity swings during the Matuyama–Brunhes (M–B) transition from two high-resolution loess–palaeosol records. *Journal of Geophysical Research* 115, B05101. doi:10.1029/2009JB006301.
- Yue, L.P., Zhou, Y., Wang, Y., 1990. Research of B/M polarity transition at loess section in China (in Chinese with English abstract). *Journal of Northwest University (Natural Science Edition)* 2, 63–64.
- Zhao, X., Roberts, A.P., 2010. How does Chinese loess become magnetized? *Earth and Planetary Science Letters* 292, 112–122.
- Zheng, H.B., An, Z.S., Shaw, J., 1992. New contributions to Chinese Plio–Pleistocene magnetostratigraphy. *Physics of the Earth and Planetary Interiors* 70, 146–153.
- Zheng, H.B., Rolph, T., Shaw, J., An, Z.S., 1995. A detailed palaeomagnetic record for the last interglacial period. *Earth and Planetary Science Letters* 133, 339–351.
- Zheng, H.B., Huang, X.T., Ji, J.L., Liu, R., Zeng, Q.Y., Jiang, F.C., 2007. Ultra-high rates of loess sedimentation at Zhengzhou since State 7: implication for the Yellow River erosion of the Sanmen Gorge. *Geomorphology* 85, 131–142.
- Zhou, L.P., Shackleton, N.J., 1999. Misleading positions of geomagnetic reversal boundaries in Eurasian loess and implications for correlation between continental and marine sedimentary sequences. *Earth and Planetary Science Letters* 168, 117–130.
- Zhu, R.X., Laj, C., Mazaud, A., 1994a. The Matuyama–Brunhes and Upper Jaramillo transitions recorded in a loess section at Weinan, north-central China. *Earth and Planetary Science Letters* 125 (1–4), 143–158.
- Zhu, R.X., Zhou, L.P., Laj, C., Mazaud, A., Ding, Z.L., 1994b. The Blake geomagnetic polarity episode recorded in Chinese loess. *Geophysical Research Letters* 21, 697–700.
- Zhu, R.X., Pan, Y.X., Guo, B., Liu, Q.S., 1998. A recording phase lag between ocean and continent climate changes: constrained by the Matuyama/Brunhes polarity boundary. *Chinese Science Bulletin* 43, 1593–1598.
- Zhu, R.X., Pan, Y.X., Liu, Q.S., 1999. Geomagnetic excursions recorded in Chinese loess in the last 70,000 years. *Geophysical Research Letters* 26, 505–508.
- Zhu, R.X., Liu, Q.S., Jackson, M.J., 2004. Paleoenvironmental significance of the magnetic fabrics in Chinese loess–palaeosols since the last interglacial (<130 ka). *Earth and Planetary Science Letters* 221, 55–69.
- Zhu, R.X., Liu, Q.S., Pan, Y.X., Deng, C.L., Zhang, R., Wang, X.F., 2006. No apparent lock-in depth of the Laschamp geomagnetic excursion: evidence from the Malan loess. *Science in China. Series D: Earth Sciences* 49, 960–967.
- Zhu, R.X., Zhang, R., Deng, C.L., Pan, Y.X., Liu, Q.S., Sun, Y.B., 2007. Are Chinese loess deposits essentially continuous? *Geophysical Research Letters* 34, L17306. doi:10.1029/2007GL030591.
- Zijderveld, J.D.A., 1967. A. C. demagnetization of rocks: analysis of results. In: Collinson, D.W., Creer, K.M., Runcorn, S.K. (Eds.), *Methods in Paleomagnetism*. Elsevier, New York, pp. 254–286.